Turkish Journal of Earth Sciences (Turkish J. Earth Sci.), **Vol. 13**, 2004, pp. 249-267. *Copyright ©TÜBİTAK*

Areal Distribution and Bulk Rock Density Variations of the Welded İncesu Ignimbrite, Central Anatolia, Turkey

ULRIKE MUES-SCHUMACHER[1], ROLF SCHUMACHER[1],
LOTHAR GEORG VIERECK-GÖTTE[2] & PETRA LEPETIT[2]

[1] Hauptstraße 3, D-71672 Marbach – Germany
(e-mail: ulrike.mues-schumacher@ uev.de)
[2] Institut für Geowissenschaften, Friedrich-Schiller-Universität, Burgweg 11, D-07749 Jena – Germany
(e-mail: viereck@ geo.uni-jena.de)

Abstract: The 2.8 Ma İncesu ignimbrite is one of the most densely welded ignimbrites of the Cappadocian Volcanic Province. Estimates of areal extent and volume reveal at least 7,760 km^2 and 38 km^3 of erupted magma. The source area can be located beneath the northeastern flanks of the Erciyes Dağ–Koçdağ stratovolcano. Today, the ignimbrite typically forms relatively small plateaus or isolated remnants and caps on hill tops. Field characteristics of the deposit include a local dark-brown or black basal vitrophyre and horizontally zoned changes in colour which correspond to changes in modal composition. Upwardly increasing amounts of lithic fragments and pumice are obvious in many locations. Depositional structures are scarce and visible only in places of obviously lower bulk rock density. The areal distribution is strongly controlled by palaeotopography of older volcanic cones and the Taurus forehills that channelised individual flow portions and partly terminated their runout.

Bulk rock density of the ignimbrite is as high as 2.34 g/cm^3 in the basal vitrophyre of the type section in the town of İncesu. It generally decreases upsection to 1.77 g/cm^3 at the top of the outcrop, but superposing density peaks are observed in the central and upper parts. Laterally, bulk rock densities vary systematically with increasing distance from source and in relation to palaeotopography: depositional lobes which are not terminated by topographic barriers show a consistent decrease in bulk rock density, from proximal dense to distal incipient welding. Those lobes, which are deposited against obstacles, show an unexpected re-increase in bulk rock density in front of the barrier.

The amount of crystals and lithic fragments is unimportant in the determination of bulk rock density such that the multiple density peaks represent zones of higher degrees of welding. The observed vertical pattern can be explained by the model of a compound cooling unit made up of several emplacement units which are separated from each other by pauses in the depositional sequence. Welding of the İncesu ignimbrite is thought to have resulted from compaction welding after the flows came to rest. A gas retention regime may have promoted re-dissolution of volatiles into the ashy matrix and thereby the formation of the basal vitrophyre in the type section and the frequent occurrence of the highest densities in the lower parts, respectively. The model also explains high bulk rock densities in front of topographic barriers which may have formed by local overthickening due to partial back flow and, thus, increased load pressure.

Key Words: Cappadocia, ignimbrites, welding, rock density

Kaynaşmış İncesu İgnimbiritinin Bölgesel Dağılımı ve Kayaç Yoğunluğu Değişimleri, Orta Anadolu, Türkiye

Özet: 2.8 My yaşındaki İncesu ignimbiriti Kapadokya Volkanik Bölgesinin çok iyi kaynaşmış ignimbiritlerinden birisidir. Bölgesel yayılım ve hacim tahminleri en az 7,760 km^2 ve 38 km^3'lük magmanın püskürdüğünü ortaya koymaktadır. Bu ignimbiritin kaynağı, Erciyes Dağ–Koçdağ kompozit volkanının kuzeydoğu kanadının altında yer almaktadır. Günümüzde, ignimbiritler küçük platolar, kalıntı tepecikler ve tepelerde örtüler oluşturmaktadır. Yersel koyu kahverengi veya tabandaki siyah camsı doku ile kaya bileşimine bağlı olarak gelişen yatay kuşaklar halindeki renk değişimleri ignimbiritlerin arazi özelliklerini içermektedir. İgnimbiritlerin üst seviyelerine doğru litik tane ve pomza miktarındaki artışlar bir çok yerde açıkça gözlemlenmiştir. İgnimbiritlerin çökelimiyle ilgili yapılar nadir olarak gelişmiş olup, genelde kayaç yoğunluğunun az olduğu alanlarda gözlemlenmişlerdir. İgnimbiritlerin bölgesel dağılımı, her bir akıntıyı kanalize eden veya akıntıların önünü kesen volkanik koniler ile Toros Dağlarının paleocoğrafyası tarafından etkin olarak kontrol edilmiştir.

İncesu kasabasındaki tip kesitinin taban kesimlerinde ignimbiritlerin kayaç yoğunluğu 2.34 g/cm^3 kadar yükselebilmektedir. Yoğunluk üst kesimlere doğru 1.77 g/cm^3 ye kadar düşmekte, ancak tip kesitin orta ve üst bölümlerinde yüksek değerlere ulaşmaktadır. Kayaç yoğunluğu yanal olarak kaynaktan uzaklaştıkça ve paleotopografyaya bağlı olarak sistematik bir değişiklik gösterir: topoğrafik bariyerler tarfından engellenmeyen çökelim lobları kayaç yoğunluğunda sabit bir azalma – proksimal alanlarda daha yoğun, ırak kesimlerde ise az

kaynaşmış şeklinde bir değişim – sunarlar. Buna karşın, bariyerler tarafından engellenmiş akıntılar özellikle bariyerlerin önününde kayaç yoğunluğunda beklenmedik bir artış göstermektedir.

İgnimbirit istifi içinde gözlemlenen çok sayıda yoğunluk artışlarının kaynaşmanın belirgin/çok iyi olduğu düzeylere denk düşmesi, gerek kristal gerekse litik tanelerin miktarının kayaç yoğunluğunun belirlenmesinde çok da önemli olmadıklarına işaret eder. İstif içerisinde dikey yönde gözlemlenen yoğunluk değişimleri birbirlerinden belli bir zaman aralığı ile ayrılan çok sayıdaki akıntıdan oluşan bir istifin varlığı ile açıklanabilir. İncesu ignimbiritinin kaynaşmasının akıntının durağan hale gelmesini takip eden dönemde sıkışmaya/yoğunlaşmaya bağlı olarak geliştiği düşünülmektedir.

Gaz alıkoyma rejimi uçucu gazların kül içeren hamurda erimesini teşvik etmiş olabilir. Buda, tip kesitin tabanındaki camsı düzeyin oluşmasına ve istifin alt kesimlerinde yüksek yoğunluk düzeylerin oluşmasına neden olmuş olabilir. Önerilen model, topoğrafik bariyerlerin önünde gözlemlenen ve olasılıkla bariyere çarpan akıntının kısmende olsa geri dönmesine bağlı gelişen yersel kalınlaşma ve bunun doğal sonucu olan yüksek yük basınca bağlı oluşan yüksek kayaç yoğunluklarını da açıklamaktadır.

Anahtar Sözcükler: Kapadokya, ignimbirit, kaynaşma, kayaç yoğunluğu

Introduction

Volcanism in Turkey is closely related to closure and subduction of the Neotethys. Four major volcanic provinces developed during the Neogene and Quaternary, namely the Western Anatolian, Central Anatolian, Eastern Anatolian and Galatean volcanic provinces (Figure 1). The volcanic activity prograded from west to east with the oldest rocks in Western Anatolia. The Central Anatolian Province – extending for about 300 km in a NE–SW direction within the Anatolides – exposes the most prominent tephra series that is chiefly exposed between the Tuz Gölü and Sultansazlığı depressions. This tephra series is composed of at least 10 major and two minor ignimbrite sheets which were emplaced during the past 12 Ma (Figure 2). They are separated from each other by various products of other, less voluminous tephra eruptions, products of effusive activity, and continental epiclastic deposits such as lahars, and fluvial and lacustrine sediments (Pasquarè 1968; Innocenti *et al.* 1975; Pasquarè *et al.* 1988; Schumacher *et al.* 1990; Le Pennec *et al.* 1991, 1994; Temel 1992; Schumacher & Mues-Schumacher 1997; Toprak *et al.* 1994; Mues-Schumacher & Schumacher 1996). Although welding of tephra is not common in Cappadocia, a general increase in welding intensity of individual ignimbrites can be observed in the upper parts of the stratigraphy sequence.

With respect to the welding of tephra, the classical work by Smith (1960a & b) defines welding as that process which promotes the union or cohesion of glassy fragments, and further describes the transition from *incipient* to *complete welding* as the progressive loss of pore space and deformation of shards and pumice. *Incipient welding* in rhyolitic pyroclastic flow deposits needs conservation of minimum temperatures of 600 ± 25 °C after emplacement (Ragan & Sheridan 1972; Riehle 1973; Sheridan 1979). Recent interest has concentrated on the influence of composition, temperature, and depositional thickness on the final bulk rock density (Riehle *et al.* 1995). Streck & Grunder (1995) described the welding intensity, recrystallisation of glass shards and vapour-phase crystallization in the welded Rattlesnake Tuff ignimbrite in Oregon, U.S.A. Finally, Sparks *et al.* (1998) showed the influence of re-dissolution of volatiles into glass shards on the welding intensities of tephra deposits.

The 2.8 Ma İncesu ignimbrite constitutes the uppermost part of the Cappadocian tephra sequence (Figure 2). It is one of the most widespread and one of the most densely welded ignimbrites of central Anatolia. We therefore studied in detail its vertical and lateral variations in bulk rock density to elucidate the influence of palaeotopography, particularly the influence of topographic barriers which partly terminated the runout of the corresponding pyroclastic flows.

In the following, we maintain the stratigraphic term *İncesu ignimbrite* introduced by Pasquarè (1968) to describe a welded ignimbrite exposed around the town of İncesu. Some contributions, notably by Le Pennec *et al.* (1994) and Temel *et al.* (1998), refer to this unit as the *Valibaba Tepe ignimbrite*.

Areal Distribution

We mapped the semi-continuous distribution of the İncesu ignimbrite over an area of about 100 x 100 km, which takes in the 115 locations we have studied (Figure

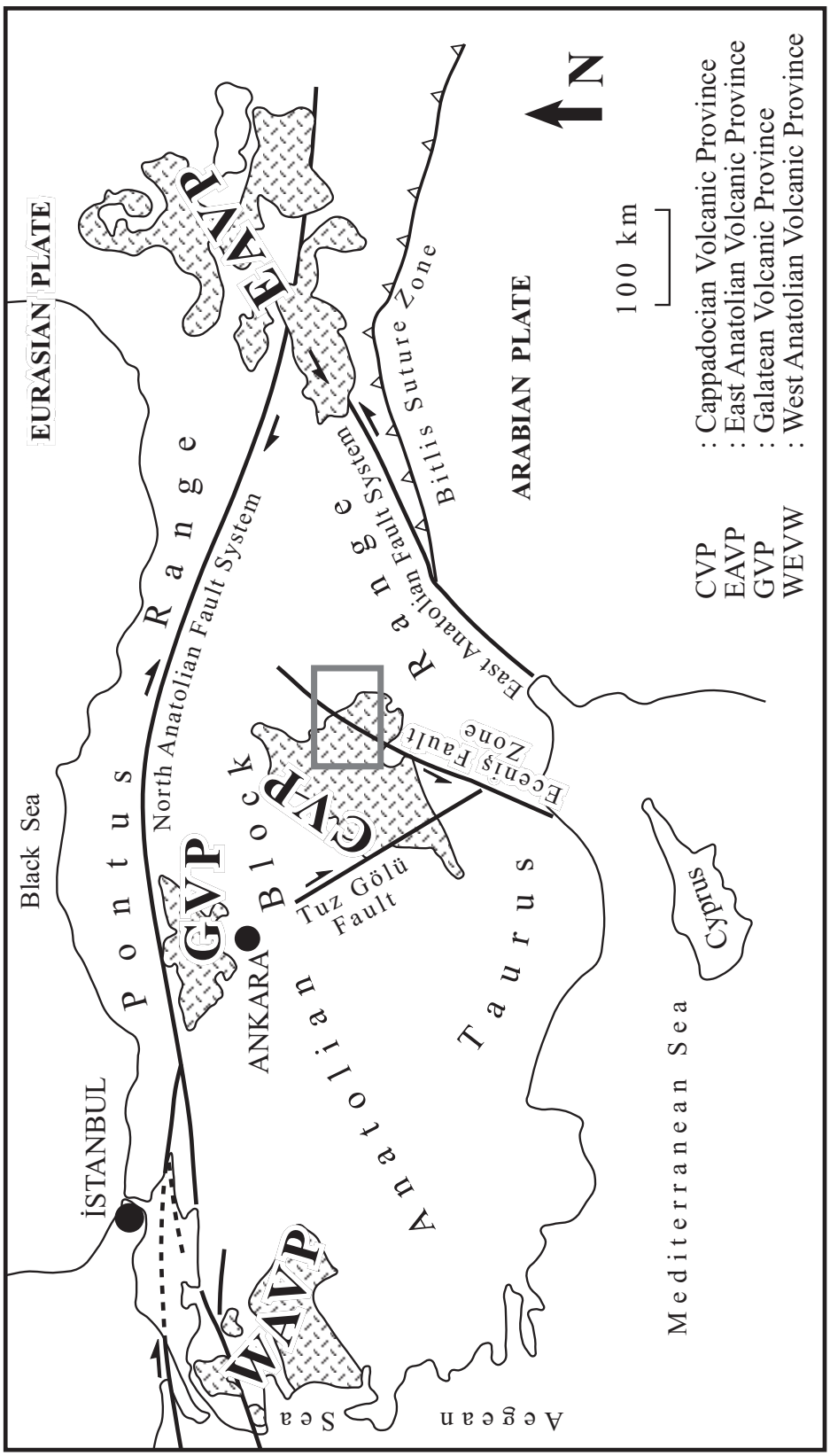

Figure 1. Geological sketch map showing the major structural features of Turkey as well as the four major volcanic provinces. The arrow and frame indicate the location of the study area in the eastern part of the Cappadocian Volcanic Province.

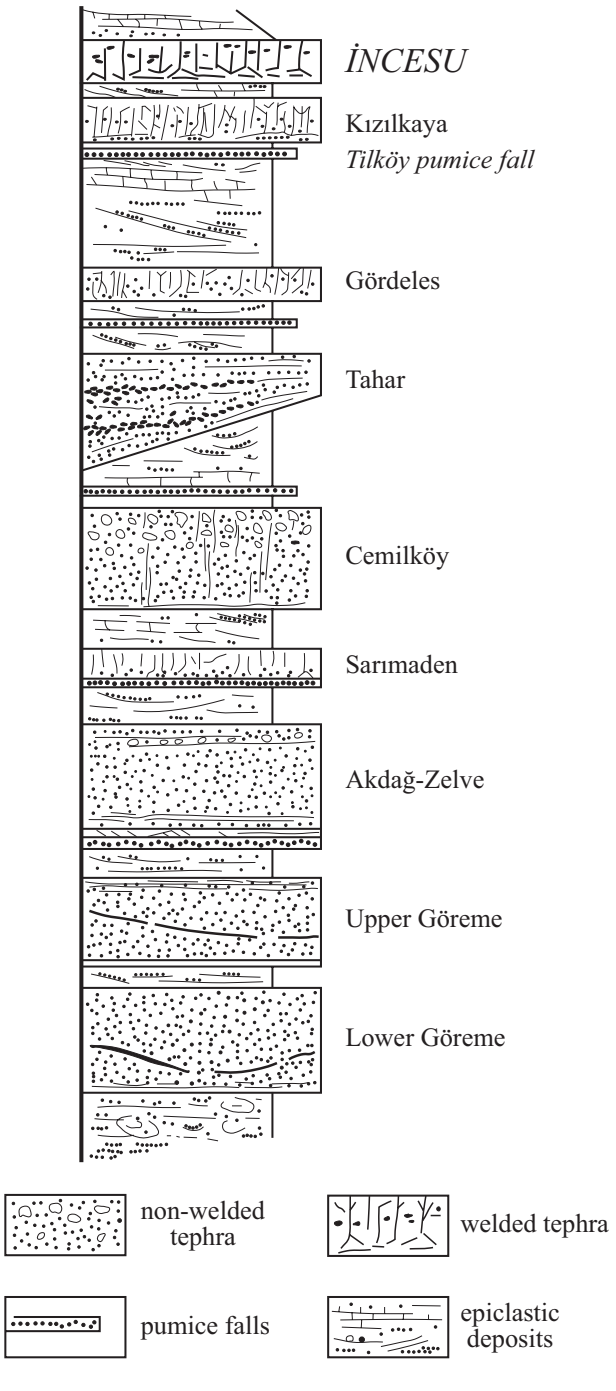

Figure 2. The generalized stratigraphic section of the Cappadocian tephra sequence showing the major ignimbrites that are interbedded with extensive epiclastic deposits. Although the Sarımaden ignimbrite is the oldest welded unit of the sequence, welding becomes important only in the upper part of the section with the İncesu ignimbrite which is the most densely welded deposit in Cappadocia.

3). The distribution area is transected by the Ecemiş Fault Zone, two feeder branches of which form a pull-apart basin – the Sultansazlığı depression – which is filled with young sediments. Limitations in field exposure are also due to a younger ignimbrite cover and the Erciyes Dağ stratovolcano; thus, we found no outcrops of the İncesu ignimbrite in the centre of the study area.

The present-day exposure constitutes an area of 595 km^2 (Table 1). The reconstructed area originally covered by the İncesu ignimbrite but later eroded or buried by younger deposits has been divided into three qualitative categories: *'certain'*, *'likely'* and *'probable'*, indicating increasing degrees of uncertainty (Table 1). The *'certain'* category includes areas connecting present-day outcrops and takes in another 385 km^2. *'Likely'* takes in 3,150 km^2 and is the most probable reconstruction of the individual flow lobes relative to topography, the proximal areas toward the assumed source area beneath Erciyes Dağ and in the Sultansazlığı depression. *'Probable'* was assigned to lobes connecting well-correlated but presently isolated distal remnants and encloses at least 1,370 km^2. Hence, the İncesu ignimbrite covered an area of 5,500 km^2, which might be the minimum value of this conservative estimate. Based on these data, a more probable reconstruction of distal lobes reveals an areal extent of about 7,700 – 7,800 km^2.

Based on these area/thickness data, we can further estimate the aspect ratio, which is the ratio of maximum thickness to runout distance, considered an indicator of the energy of an ash flow (Walker 1983). The aspect ratio of the İncesu ignimbrite is between 1:5,000 and 1:22,000, depending on conservative or optimistic estimates of 4 m / 20 km or 3 m / 66 km, respectively. Both aspect ratios are within the range of extensive, high-energy, low-aspect-ratio ash-flow tuffs.

Volume

To calculate the erupted volume, we use all thickness data with conservative minimum thicknesses of present-day exposures combined with the reconstructed distribution areas and associated thicknesses in the different categories (Table 1). A total (minimum) volume of 45.4 km^3 of welded tephra is obtained. The corresponding magma volume is less because of variations in welding intensity. Using approximate average densities in each partial volume, we obtained a total magma volume

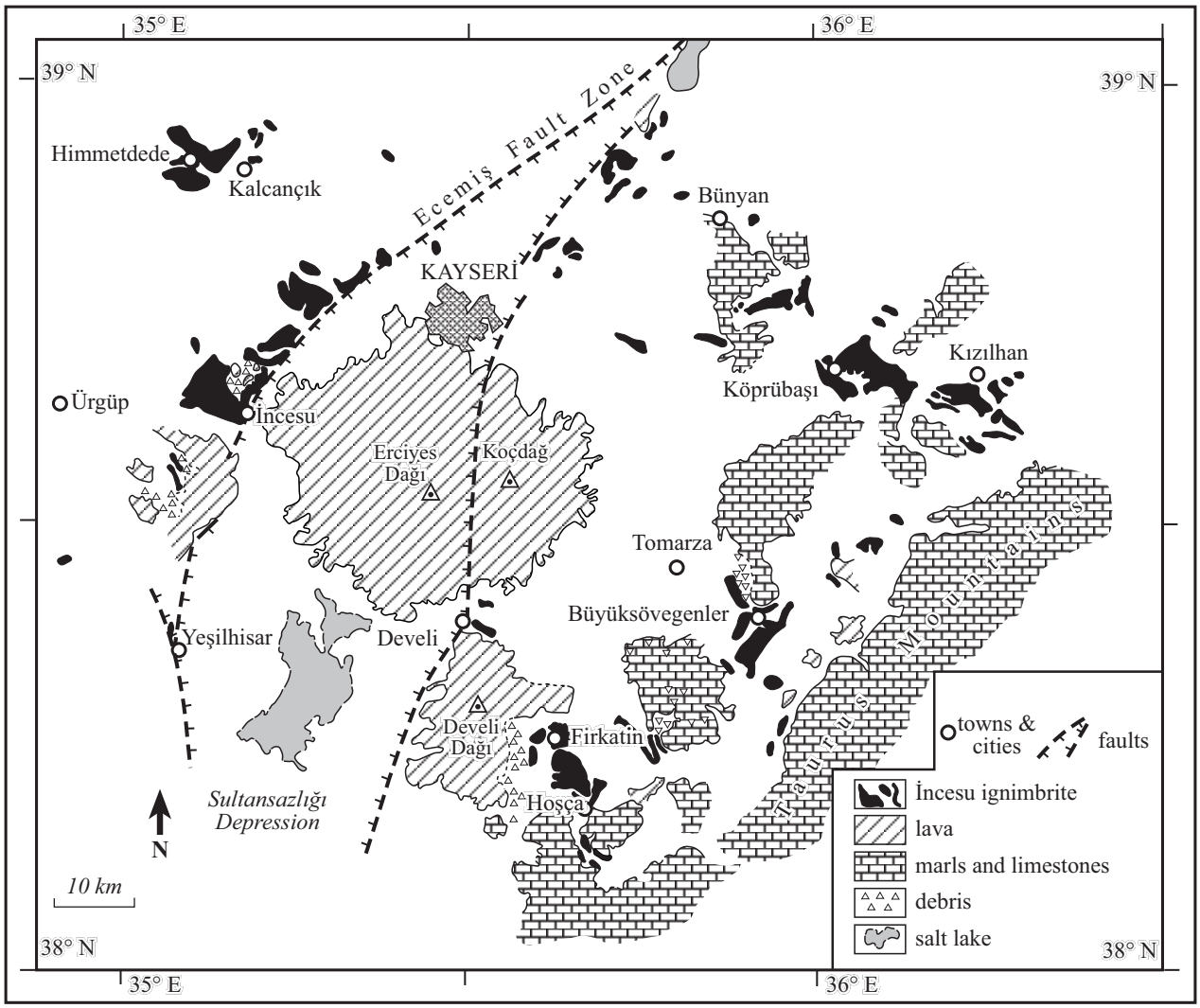

Figure 3. Geological sketch map of the study area showing the semi-continuous regional distribution of the İncesu ignimbrite. No exposures were found in the centre of the area due to faulting, young sedimentary and ignimbritic cover, and the growth of Erciyes Dağı.

erupted of about 38 km^3. This volume is on the order of the Crater Lake eruption of Mt. Mazama and the Taupo eruption (Smith 1979; Walker 1983), and less than estimates made by Le Pennec *et al.* (1994) and Temel *et al.* (1998), who supposed an areal extent of 5,200 km^2 and a tephra volume of 100 km^3 for their '*Valibaba ignimbrite*'.

Field Characteristics

The İncesu ignimbrite generally forms small plateaus (Figure 4a), a few tens of square kilometers wide, or occurs as isolated remnants and caps on or near hilltops. Outcrops typically expose 3 – 10 m of a reddish-brown ignimbrite; its thickness exceeds 15 or 20 m in only a few locations. The outcrops commonly have coarse columnar jointing with individual columns up to about 5 m in diameter (Figure 4b). Distally, particularly in the south and southeast, the İncesu ignimbrite became channelised in the valleys of the Taurus forehills that terminated the runout. In spite of the palaeotopography and channelising of flow portions, distinct valley ponds of the ignimbrite are rare. The ignimbrite lacks rheomorphic features as described from the Rattlesnake Tuff of eastern Oregon

Table 1. Area and volume estimates of the İncesu ignimbrite. The calculation of the erupted magma volume is referred to the maximum density for the basal vitrophyre of 2.35 g/cm^3.

	Area (km^2)			Volume (km^2)				Erupted magma (km^2)	
	Area	Cumulative area	Associated thickness	Ignimbrite volume	Cumulative volume	Assumed density (g/cm^3)	density ignimbrite / density vitrophyre	Volume	Cumulative volume erupted
Isopach area of present day exposure									
2 – 4 meters	169	169	3 m	0 507	0.507	1.65	0.70	0.355	0.355
4 – 7 meters	282	451	5 m	1.410	1.917	1.80	0.77	1.086	1.441
7 – 10 meters	49	500	8 m	0.392	2.309	2.00	0.85	0.333	1.774
> 10 meters	94	**594**	10 m	0.940	**3.249**	2.25	0.96	0.902	**2.676**
Reconstructed									
Certain	376	376	2 – 6 m	1.504	1.504	1.70	0.72	1.083	1.083
Likely	3,154	3,530	8 – 12 m	31.540	33.044	2.10	0.89	28.071	29.154
Probable	3,636	**7.166**	app. 2.5 m	9.090	**42.134**	1.60	0.68	6.181	**35.335**
Total		**7.760 km^2**			**45.383 km^2**				**38.011 km^2**

(Streck & Grunder 1995) or the Gribbles Run palaeovalley tuff of central Colorado (Chapin & Lowell 1979).

The İncesu ignimbrite typically lacks basal pumice fallout deposits, in contrast to most of the other ignimbrites of the Cappadocian Volcanic Province. Two locations, however, location 115 near Büyüksövegenler (Figure 5a) and location 103 near Kızılhan, show 1.5 – 8 cm of a whitish material beneath the ignimbrite that could be interpreted as strongly altered and weathered pumice fallout.

The Type Section of İncesu Ignimbrite

The type section of the İncesu ignimbrite, location 4 at the western margin of the town of İncesu, is composed of about 27 – 28 m of densely to incipiently welded ignimbrite (Figure 4c) and subdivided into three individual zones that can be identified by differences in colour, concentrations of crystals, pumice, and lithic clasts as well as by density (Mues-Schumacher 1997).

The *basal unit* is a dark-brown or black vitrophyre, about 1 m in thickness and includes about 25 cm of pale buff-coloured loose material at its base. Thin sections show radial fibrous whiskers of clay minerals and some preserved Y- and T-shaped glass shards, indicating that the loose material is primarily non-welded ash. The basal vitrophyre is overlain by a bright-red to dull brick-red densely welded *central unit*. Up section, the colour grades through brownish-violet or dark pinkish grey into pale grey within the *upper unit* of the İncesu ignimbrite. The welding intensity of the İncesu ignimbrite decreases from the bottom to the top of the deposit, as is obvious from flattening ratios and the vesicularity of pumice clasts (see also Peterson 1979), the degree of which increases upwardly. Pumice clasts are extremely flattened in the basal vitrophyre and the lower central unit. Higher up, the decrease in flattening can be documented by M_{P7}-values (average flattening ratios of the seven most-flattened pumices of a stratigraphic level). Throughout the uppermost 15 m of the İncesu ignimbrite, M_{P7} decreases from 8.85 in the pinkish-grey zone to 4.31 at the top of the outcrop (Figure 6).

The amount of crystals and lithic fragments also changes with stratigraphic position, corresponding to the change in colour. The basal vitrophyre has 2 – 5 volume % of phenocrysts, but the amount abruptly increases to 8 – 15 volume % up-section at the transition to the central red unit (Lepetit 1999). Lithic fragments are generally scarce within the basal vitrophyre, whereas a few small pieces were found in the central unit. Throughout the upper unit, the lithic-fragment content increases significantly to about 10 volume %, and the size of the fragments increases correspondingly; the M_{L5}-value (average diameter of the five largest lithic fragments of a stratigraphic level) increases within the upper units from

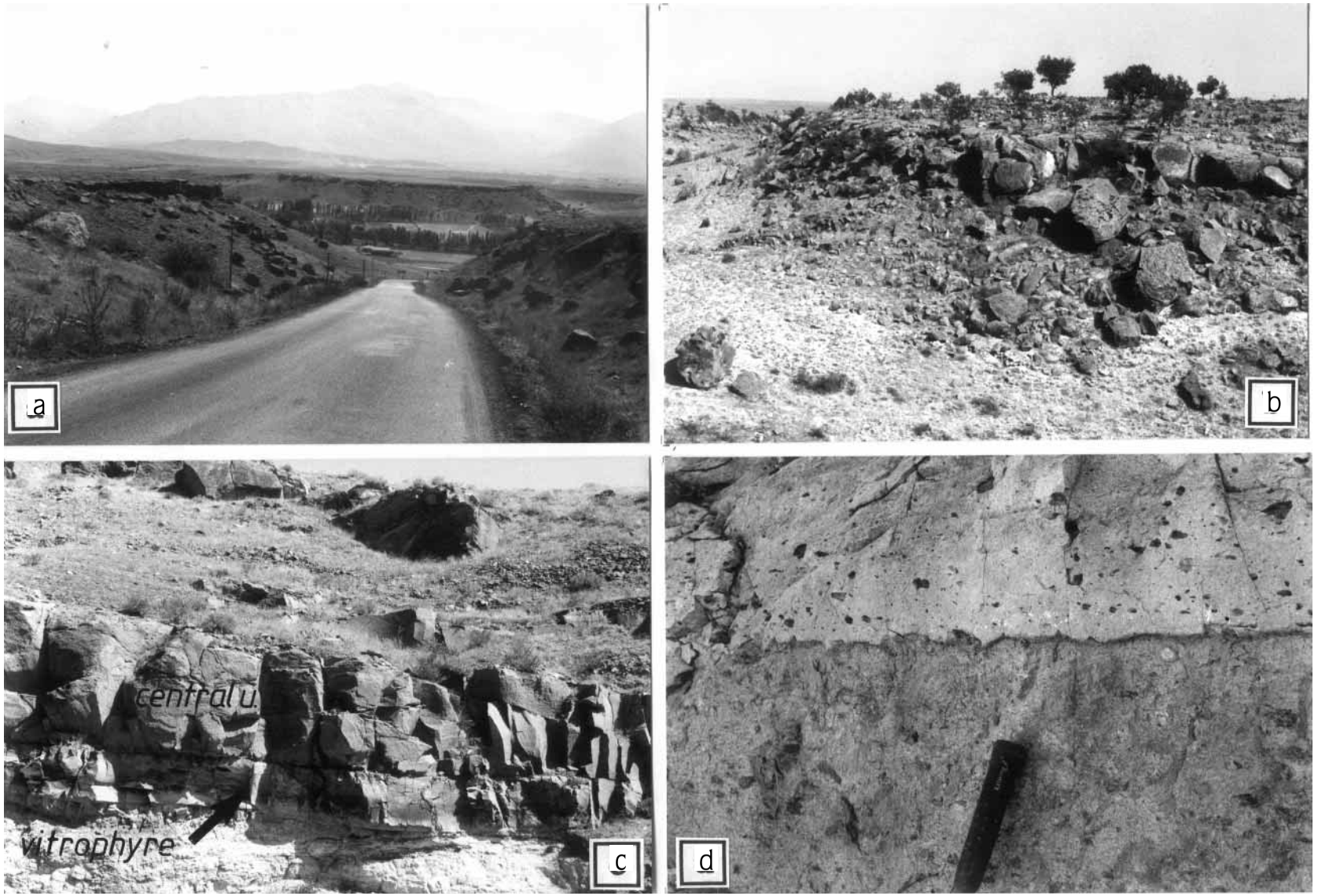

Figure 4. Photographs illustrating some field characteristics of the İncesu ignimbrite. **(a)** The İncesu ignimbrite forms a small plateau between the Taurus forehills around the village of Büyüksövegenler (location 14); **(b)** plateau of the İncesu flow lobe west of the type location: the ignimbrite shows wide-tracked, square columnar jointing (location 18); **(c)** the İncesu type section (location 4) at the western margin of the town of İncesu exposes the dark-brown/black basal vitrophyre; **(d)** close-up view of typical boundary between the lower dark-grey basal unit and the dull brick-red central unit in incipiently or intermediately welded sections.

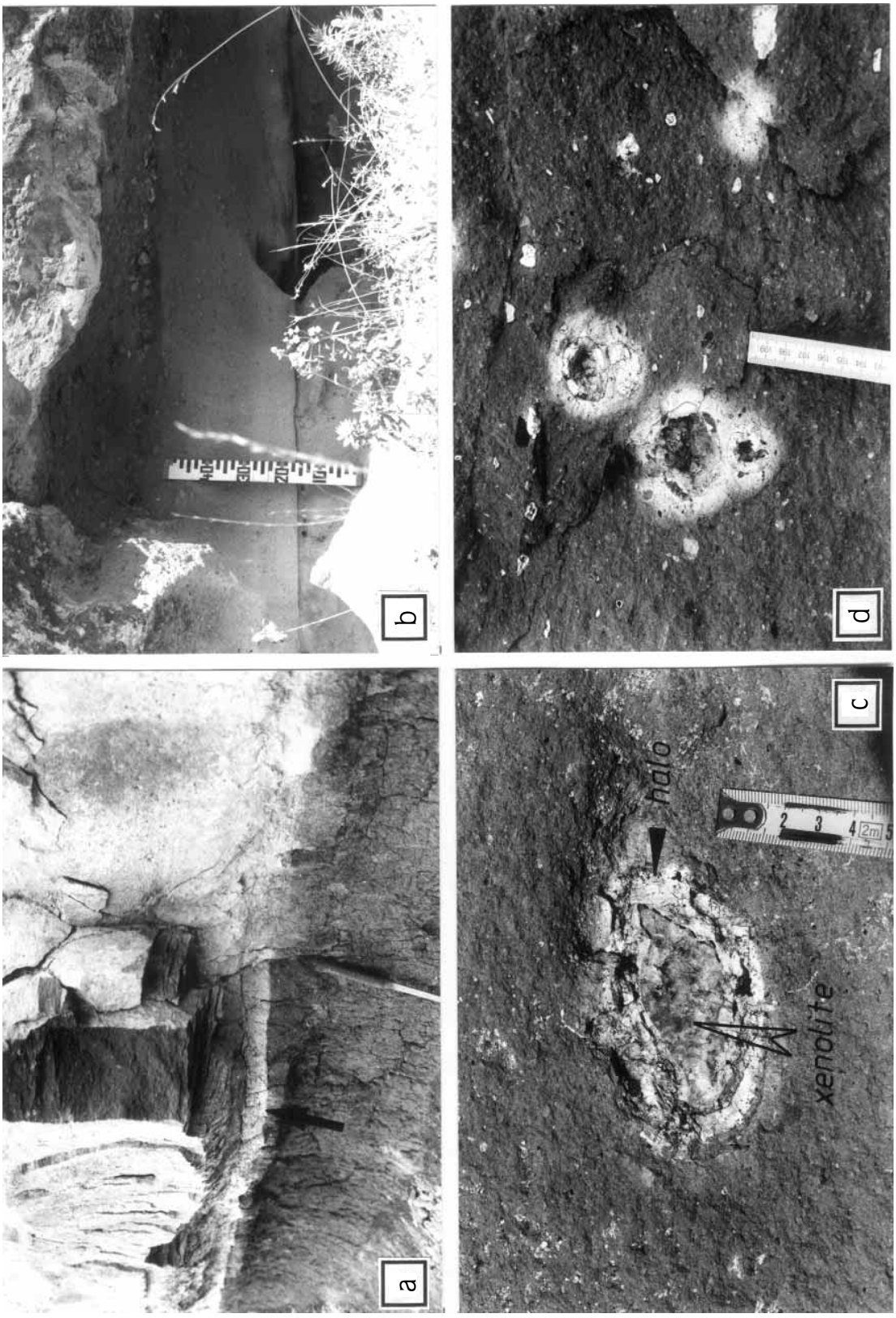

Figure 5. Photographs illustrating some internal characteristics of the İncesu ignimbrite. **(a)** Location 115 northeast of Büyüksövegenler exposes 5 cm of whitish loose material beneath the ignimbrite which could be interpreted as thin initial pumice fall of the eruption; **(b)** lithic segregation layers within the basal unit at location 97 near Köprübaşı. Tephra is only incipiently welded within the basal unit. The vertical bulk rock density profile is independent of the lithic layers but density increases rapidly above the lithic layers from 1.49 g/cm^3 to 1.66–1.71 g/cm^3 – see Figure 10 for density profile; **(c)** halo formed around a carbonate xenolith which was tempered by the ignimbrite and transformed into marble. The halo appears as a reaction rim of the rock fragment and the silicic ignimbrite tephra; **(d)** yellowish to greenish-white *haloes* frequently found in the Himmetdede quarries (location 23). They have developed within the central and upper units of distal, incipiently welded deposits.

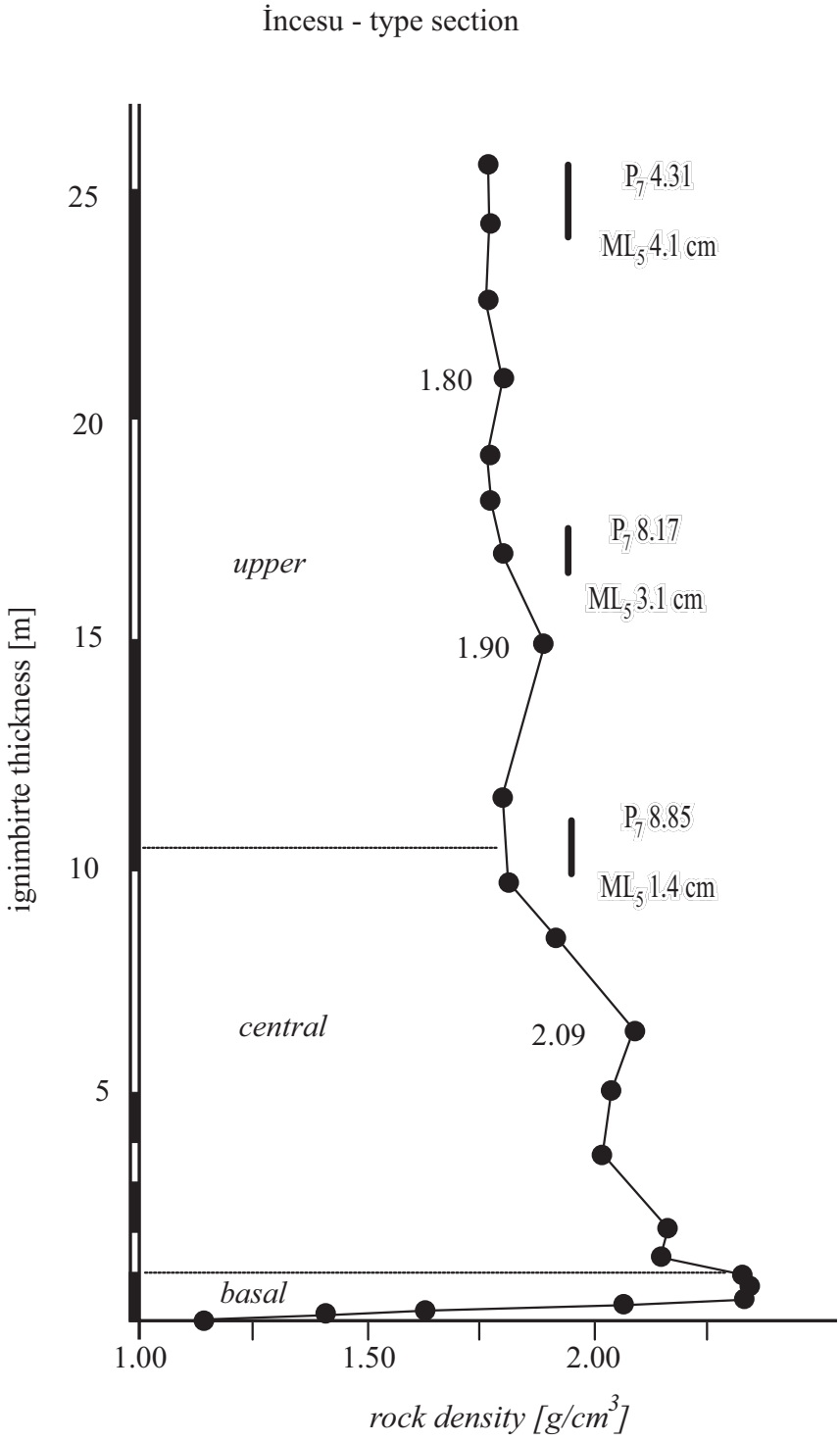

Figure 6. Bulk rock density variation of the type section. Note the steep basal density gradient and the general upward decrease that is superposed by different peak density values in the central and upper parts; P_7 – values denote the aspect ratios (maximum length/maximum width) of the seven largest pumices, M_{L5} – values denote the mean of the five largest lithic fragments.

M_{L5} = 13.8 mm in the pinkish-grey part to M_{L5} = 40.6 mm at the top of the outcrop.

In addition, yellowish to greenish-white haloes with maximum diameters of up to 40 mm can be found in the middle of the upper unit, ~ 15 to 22 m above the base; these features are either cored by small lithic particles or their interiors are hollow. These haloes commonly appear as alteration or reaction rims around hydrothermally altered wall-rock fragments that partly caused breakdown of the surrounding ignimbrite material (Figure 5c & d).

Lateral Variations

Generally, the internal fabric of the İncesu ignimbrite varies from dense welding in the proximal facies to incipient welding and non-welding distally. The basal zone, however, is vitric only at a few isolated locations. The vertical subdivision based on changes in colour can be identified almost throughout the study area except for the southern (Firaktin-Hoşca area) and southeastern lobes (Büyüksövegenler area). The reddish colours of the central part are mostly absent here; the dark basal zone, locally as thick as 3 m, is almost directly overlain by violet-pinkish-grey ignimbrite portions which we consider to represent the upper units.

The lithic-fragment content locally varies significantly; local incorporation of loose debris picked up from the ground can be observed at several places. An overall higher lithic-fragment concentration in the basal segment was observed in the southern lobe. Part of the increase may be attributed to local incorporation of debris, but the overall scatter of particles 1 – 3 cm in size is attributed to primary effects of higher lithic-fragment contents in these particular ignimbrite horizons.

The distribution of haloes appears to be more or less arbitrary because no regional distribution pattern or relation to distinct stratigraphic positions was perceived. The highest amounts were found in location 23, the *Himmetdede quarries*, within the upper half of the deposit (Figure 5d). Location 38, *Kalcancık*, shows an irregular scatter of haloes over the entire section and thus rules out the possible relationship to distinct stratigraphic levels. Similar relations were observed in the southern Firaktin-Hoşca lobe, where locations 88 and 89, in particular, also have high concentrations.

Primary depositional structures, such as lithic- and pumice-fragment concentration layers characterising individual flow units, are absent in levels of dense welding or were partly obscured by the welding. They were observed, however, at several places between Bünyan and Kızılhan that show an overall lower degree of welding (Figure 5b). A striking example was found in location 97, *Köprübaşı*, showing two distinct lithic-fragment concentration layers in the basal unit. Moreover, concentrations of undeformed, highly vesicular pumice clasts in location 108 are exposed in the same general area.

Degassing pipes, which are well known from the stratigraphically lower, less intense welded Kızılkaya ignimbrite (Schumacher & Mues-Schumacher 1996), are almost absent in the İncesu ignimbrite, which may also have been obscured by welding. The only known exception occurs in the distal Himmetdede quarries (location 23): elongated vertical pipes – which are often similar to haloes (yellowish-green rims) – were interpreted as gas-escape pipes.

Source Area

By analogy with similar erupted magma volumes of roughly 50 km^3, a small ring structure with caldera subsidence between 5 and 10 km in diameter might be expected. However, no such structure is exposed and, thus, positioning of the source area of the İncesu ignimbrite is rather difficult. Standard means, such as thickness distribution of initial pumice-fall deposits, internal depositional structures, or the decrease/increase relationships and size distribution of lithic clasts, do not work. Pasquarè (1968) and Le Pennec *et al.* (1994) quite generally supposed the Kayseri region to locate the source area. Kürkcüoğlu *et al.* (1998) centred the İncesu ignimbrite beneath Koçdağ, which forms the eastern flank of the Erciyes Dağı stratovolcano. Those authors placed the ignimbrite with subsequent caldera subsidence stratigraphically at the end of the Koçdağ stage and at the beginning of the neo-Erciyes stage in the evolution of Erciyes Dağı.

Bulk rock density data, combined with the assumed spreading paths of the pyroclastic flows – which were deduced from field observations and a series of topographical cross-sections that we combined to a tree-dimensional block diagram – suggest that the source area

can be located beneath the eastern part of the Erciyes Dağı/Koçdağ stratovolcano in the vicinity of the eastern branch of the Ecemiş Fault Zone (Figure 7).

Variations in Bulk Rock Density

Analytical Methods and Influence of Modal Composition and Porosity

More than 1200 bulk rock density measurements of about 900 samples were performed to study the vertical and lateral density variation of the İncesu ignimbrite. The size of the rock fragments used were 3 – 8 cm and 25 – 250 g. We used the method of water immersion after paraffin coating. All measurements were carried out at room temperature with densities of water and paraffin of 1.0 g/cm^3 and 0.86 g/cm^3, respectively. The precision of the method deduced from multiple measurements of the same sample is about ± 1.5 % and is thus similar to the range of the density (in)homogeneities of the ignimbrite itself. Two or three hand specimens from the same stratigraphic level of a section show a general density variation on the order of ± 1 %, but rare deviations are as great as 4 %.

We further analysed the influence of modal composition, lithic-fragment content, and porosity of the İncesu ignimbrite on the bulk rock density variation at the type location (Lepetit 1999; Viereck-Götte *et al.* 2001). Specific densities of the phenocrysts were deduced from

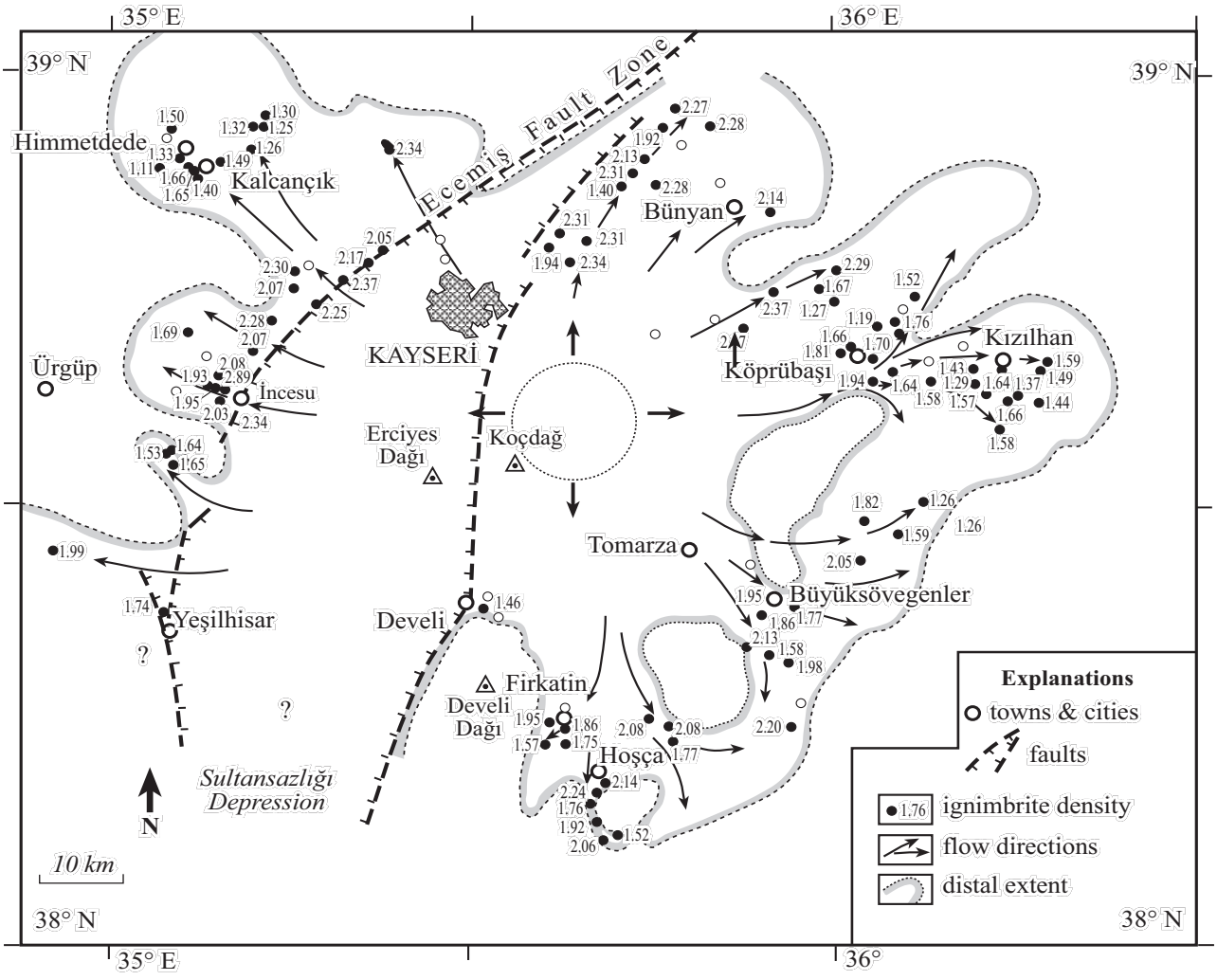

Figure 7. Sketch map illustrating the reconstructed areal extent, flow paths and source area of the İncesu ignimbrite; bulk rock density values refer to the basal unit.

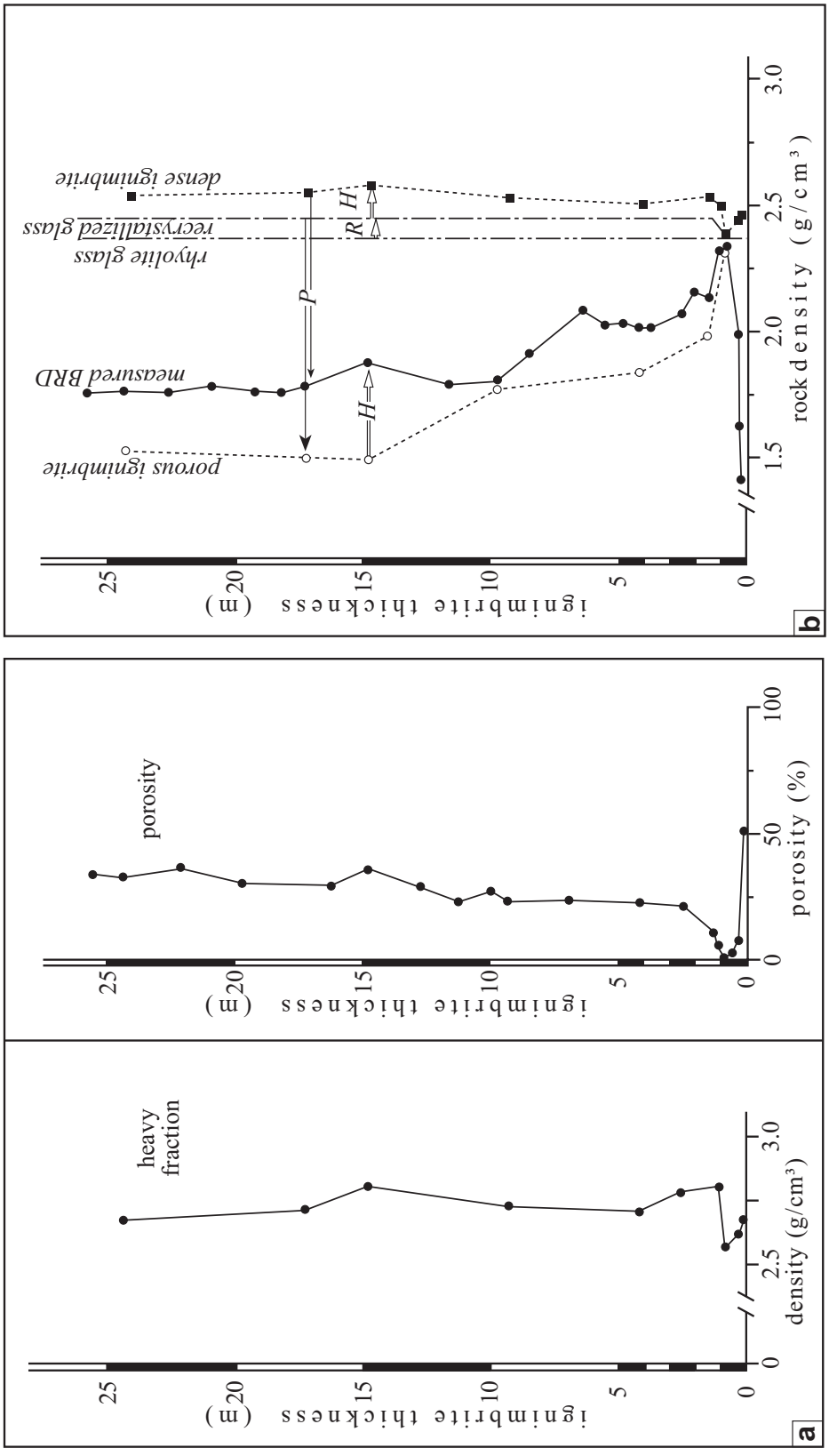

Figure 8. Vertical variations of density and porosity of the İncesu ignimbrite at the type section in İncesu. (**a**) the density variations of the specific heavy fraction (crystals and lithic components in their modal proportions) of the ignimbrite and the vertical variation of porosity; (**b**) results of model calculations to quantify the specific influence of the heavy fraction and the porosity on the measured bulk rock density. *Porous ignimbrite* denotes density of tephra samples devoid of the heavy fraction (glass recrystallised) and *dense ignimbrite* denotes tephra sample devoid of any porosity. Arrows H, P, and R describe the respective shift in density due to adding the heavy fraction (H), due to recrystallisation of glass (R), and considering the porosity (P).

their optical properties and chemical compositions: plagioclase 2.68 g/cm^3, orthopyroxene 3.55 g/cm^3, clinopyroxene 3.40 g/cm^3, and titanomagnetite 4.89 g/cm^3. The densities of five different types of lithic components were between 2.09 and 2.70 g/cm^3. We combined phenocrysts and lithic fragments in their modal proportions into a *heavy fraction* and calculated the weighted average densities, which were between 2.57 and 2.82 g/cm^3 (Figure 8a). The glass shards were analysed by EDS resulting giving a rhyolitic composition of 71.8 – 72.1 wt% SiO_2 for which we adopted an average density of 2.37 g/cm^3. XRD analyses of recrystallised glass indicate the formation of quartz, cristobalite, tridymite and sanidine. Due to their estimated modal proportions an average density of 2.45 g/cm^3 can be assumed. Porosity was measured by allowing the dried samples to imbibe isopropanol for 16 hours; the results were plotted versus height in stratigraphy.

Bulk rock density and porosity are inversely related; i.e., the minimum porosity occurs within the basal vitrophyre where the rock density is highest, and a constant upward increase in porosity is superposed by two minima in the upper half of the section (Figure 8a). For further evaluation of the influence of porosity, modal composition, and recrystallisation, two model calculations were performed: (i) We simply subtracted the specific heavy fraction, the influence of which on rock density is +0.04 g/cm^3 in the basal vitrophyre and +0.37 g/cm^3 in the upper section. Thus we obtained a hypothetical *porous ignimbrite* devoid of heavies (Figure 8b); (ii) The second calculation started at the dense glassy matrix supposing a pure vitric rock devoid of heavy components and porosity. The rock density then corresponds to rhyolite glass of 2.37 g/cm^3. Its recrystallisation would produce an average rock density of 2.45 g/cm^3 and, thus, an increase of +0.08 g/cm^3. Adding the specific heavy fraction, a hypothetical *dense ignimbrite* of 2.39 g/cm^3 is calculated from the basal vitrophyre, and of 2.54 – 2.59 g/cm^3 higher up; i.e., an increase in rock density between 0.09 and 0.17 g/cm^3 relative to pure rhyolite glass.

To summarise, the modelling illustrated in Figure 8 shows that heavy components and recrystallisation will increase the density between +0.17 g/cm^3 and +0.37 g/cm^3 relative to pure rhyolite glass, but the influence is negligible relative to the counteracting influence of porosity. This observation corresponds to the description by Smith (1960a & b) who found the transition from incipient to complete welding as progressive loss of pore space. It further shows that bulk rock density data uncorrected for crystals and lithic fragments are valid to describe variations in welding intensities.

Vertical Variations in Density

Bulk rock densities vary between 1.15 g/cm^3 and 2.34 g/cm^3 in the type section in the western outskirts of the town of İncesu (Figure 6). The lowest density of 1.15 g/cm^3 was obtained from loose material at the very base of the ignimbrite. Bulk rock density rapidly increases to 2.07 g/cm^3 40 cm above the base and to a density maximum of 2.34 g/cm^3 in the basal vitrophyre, which is also the highest value of the entire section detected 80 cm above the base. Up section, the density patterns for the central and upper units show a general decrease, from 2.34 g/cm^3 to 1.77 g/cm^3 at the top of the outcrop. This general decrease is superposed by at least three minor density peaks: the first one in the upper half of the central unit and two more in the upper units.

Moreover, the western area of the İncesu ignimbrite has its maximum density in the basal (vitric) unit or at the base of the reddish central unit whereas, in the southern and southeastern distribution areas, the maximum densities were found within the upper units.

Lateral Variations in Density

In general, maximum densities between 2.20 and 2.35 g/cm^3 were observed in (proximal) locations around the Erciyes Dağı stratovolcano, whereas (distal) locations away from Erciyes Dağı have maximum densities of 1.40 to 1.70 g/cm^3 (Figure 7). These regional density distribution patterns and lateral gradients are complicated by anomalies of unexpected higher or lower bulk rock densities, particularly between the forehills of the Taurus Mountains which have controlled the runout and emplacement of the ignimbrite. Three specific areas are discussed in detail.

(1) The northwestern Himmetdede-lobe (Figure 7) shows a constant decrease in the maximum density of the basal unit along the assumed spreading axis, from 2.37 g/cm^3 in proximal locations at the western margin of the Sultansazlığı Depression, to

1.50 g/cm^3 in distant places around the town of Himmetdede. This distance is about 27 km and the topography rises by about 100 m. A decrease in maximum density is also obvious perpendicular to the spreading axis; i.e., the density decreases from 1.66 g/cm^3 in the centre to 1.25 – 1.30 g/cm^3 in the lateral outer parts of the lobe. Regional thickness distribution, depositional facies as well as present-day morphology indicate that the runout and emplacement of the pyroclastic flows were not affected by palaeotopography.

Similar observations of a constant decrease in density have also been made elsewhere, for example, west of İncesu where topography rises from 1090 to 1200 m above mean sea level (a.m.s.l.) within about 5 km. Bulk rock density decrease from 2.34 g/cm^3 in the type section to 1.93 g/cm^3 atop a small plateau. Moreover, between the villages of Köprübaşı and Kızılhan in the northeastern lobe, bulk rock density decreases from 1.94 g/cm^3 to 1.66 – 1.44 g/cm^3. Palaeotopography of the area partly deflected flow portions from northeasterly to more easterly directions but did not terminate the runout by barriers which could not be overtopped.

(2) Contrasting the examples above, the southern distribution lobe of Firaktin – Hoşca is limited in areal extent by the volcanic rocks of the Develi Dağ in the west and by calcareous rocks of the Taurus forehills in the east and south (Figures 3 & 9). The pyroclastic flows entered a narrow channelising valley south of the village of Hoşca leading 200 m uphill to the *Hoşca Pass* (1580 m a.m.s.l.), which was overtopped so that the distal flow came to rest beyond the pass in the south. To illustrate density variations with increasing distance from source, data from the basal unit were plotted on a cross-section that parallels the spreading direction (Figure 9). The ignimbrite platform around Firaktin and particularly in Hoşca shows a rather high density of 2.14 g/cm^3 to 2.24 g/cm^3 (1386 m a.m.s.l.). A constant uphill decrease down to 1.76 g/cm^3 was observed on the northern slope at an elevation of 1513 m, and a re-increase in bulk rock density to 1.92 g/cm^3 was found in location 88 beyond the Hoşca Pass on its southern slope where the basal unit is thickest. Locations 89 and 109 presently mark the distal end of the lobe in the field. They differ completely from each other: location 109 – at the foot of a mountain terminating the runout of the pyroclastic flows – shows a density as high as 2.06 g/cm^3, whereas location 89 beside the spreading axis of the flow only shows a maximum density of 1.52 g/cm^3.

Similar features were observed in the southeastern Çulha-Büyüksövegenler lobe (Figure 7). Bulk rock densities are highest at the distal ends of the flows on the stoss-sides of topographic barriers terminating the flows, whereas a constant decrease in density occurs laterally along the barriers.

(3) Another density anomaly occurs within the ignimbrite sheet north of the village of Köprübaşı. Locations 98 and 108, NW and NE of Köprübaşı, respectively, expose a thick basal unit of incipiently welded or loose tephra showing lithic- and pumice-fragment concentration layers. In relation to the runout distance, the observed bulk rock densities of 1.19 g/cm^3 (location 98) and 1.27 g/cm^3 (location 108) from the basal unit are much too low and are surrounded by deposits of significantly higher densities in the range of 1.66 g/cm^3 (location 97) and 1.81 g/cm^3 (location 30; Figure 10). Correspondingly, preserved glass shards are largely undeformed and pumice clasts are significantly less elongated so that M_{P5}-values of 2.82 (location 98) and 2.66 (location 108) contrast with the M_{P5}-value of 5.88 within the upper part of the basal zone at location 116 (Figure 10).

To shorten the following discussion, we invoke a model similar to the non-welding of portions of the stratigraphically lower Kızılkaya ignimbrite (Schumacher & Mues-Schumacher 1996): formation of well developed lithic- and pumice-fragment concentration layers at the base of and atop individual flow units indicate dilution of individual flow portions to promote this particle segregation. The dilution, in turn, may result from enhanced fluidisation and thereby enhanced heat

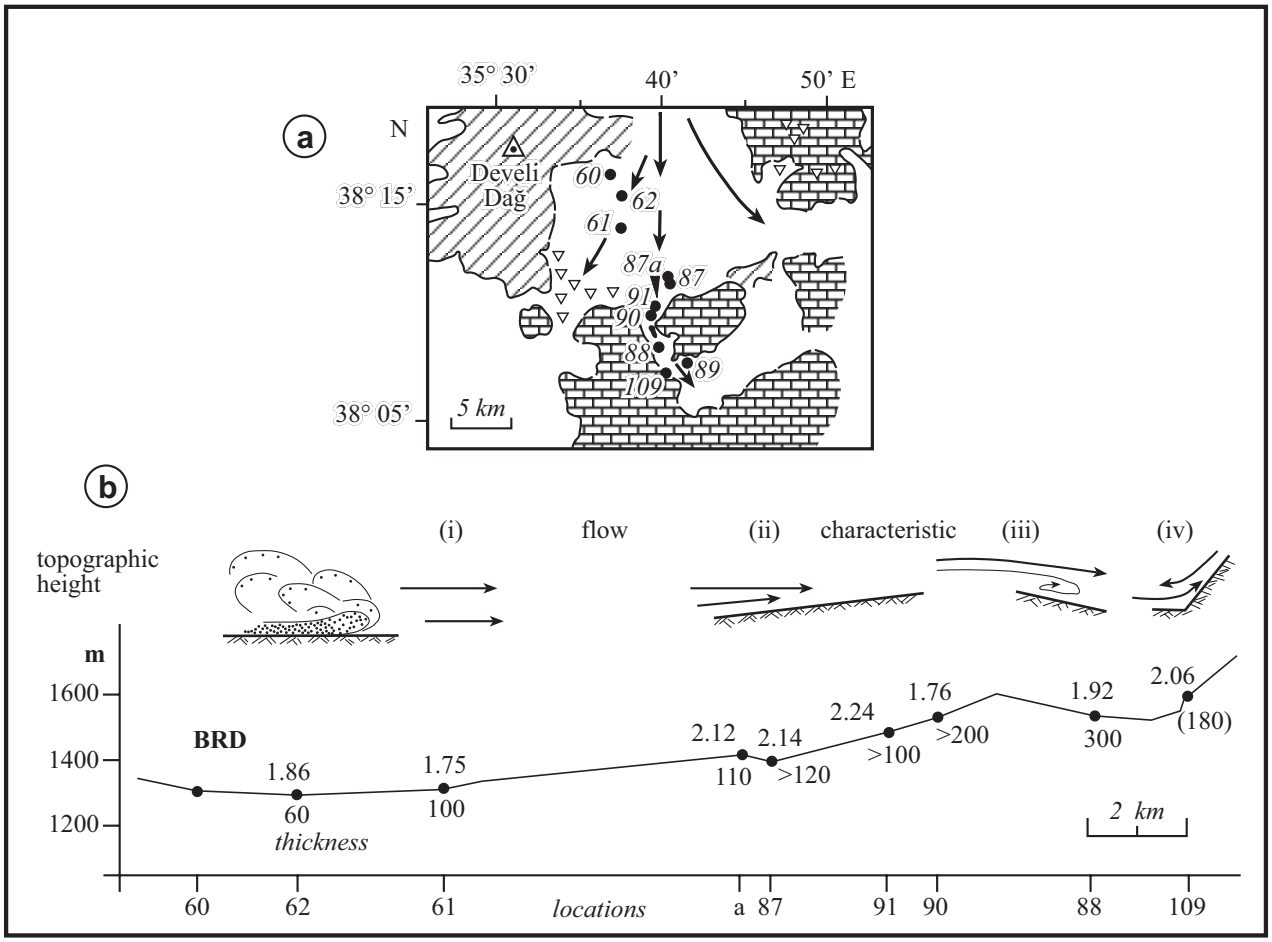

Figure 9. (a) Detailed sketch map of flow paths and (b) longitudinal cross-section of the southern Firaktin-Hoşca – lobe that overtopped the Hoşca Pass. Figures in the map and along the x-axis of the cross-section denote sample locations. The cross-section further shows the thickness of the basal unit in cm and the corresponding maximum bulk rock density (BRD) in g/cm. (i) The pyroclastic flow covers even ground around Firaktin; (ii) topography rising toward the Hoşca Pass caused some compression of the flow so that the rock density is higher at the foot of the slope; (iii) the flow portion which overtopped the pass probably became diluted and partially turbulent behind the *edge* of the pass that resulted in thickening of the deposit in location 88 and correspondingly in slightly higher rock densities; (iv) the flow was stopped in front of the topographic barrier of location 109: partial backflow from the upper slopes of the barrier caused overthickening and thereby an increase in rock density at the distal end of the flow.

exchange between the ash particles and the fluidising gas that the tephra was cooled quickly down to or even below the minimum temperature of welding.

Interpretation and Discussion

Vertical Welding Patterns

Many well known ash-flow sheets, like the Rattlesnake Tuff (Streck & Grunder 1995), the upper Bandelier Tuff (Smith & Bailey 1965), or the Bishop Tuff (Ragan & Sheridan 1972) show a single density maximum mostly in the upper part of the lower half of the deposit. This is generally interpreted as a result of temperature and especially compaction of a simple cooling unit which was theoretically confirmed by the modelling of Riehle (1973). He included the initial depositional thicknesses, emplacement temperatures, and the depositional environment in his computations.

Such a general model, however, is not adequate to explain the observed welding pattern of the İncesu ignimbrite that shows various highs and lows in welding intensity. Riehle *et al.* (1995) presented an improved

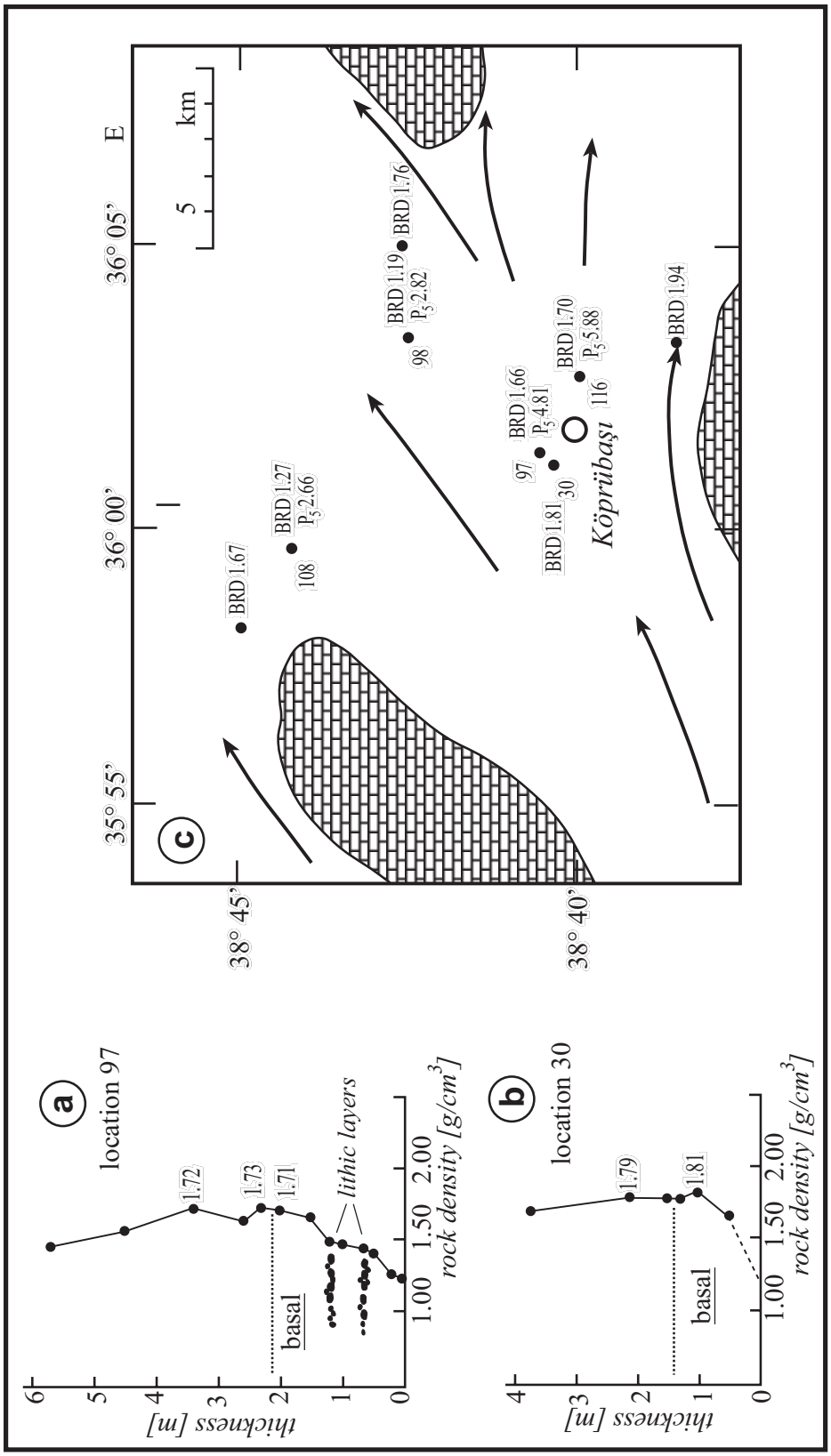

Figure 10. Anomalous low bulk rock density was detected in the area north of the village of Köprübaşı: (a) bulk rock density variation of location 97 which exposes two lithic concentration layers within the basal unit where the rock density is lowest; (b) for comparison, the bulk rock density variation at location 30 is shown – the location exposes a completely incipiently welded section without any particle segregation layers; (c) the detailed sketch map illustrates the assumed flow paths and the maximum bulk rock density in g/cm^3. P5 denotes the mean aspect ratios of the five largest pumice clasts. Note the rapid decrease in maximum bulk rock density of the basal unit within less than 1 km – the formation of lithic concentration layers in location 97 indicates local turbulence within the flow which is made responsible for cooling of tephra by enhanced heat exchange between air and tephra particles. This temperature loss during emplacement caused a lower degree of later welding than was found in surrounding locations 30 and 116.

model that evaluates compound cooling units and a variety of additional factors controlling the final density pattern of an ignimbrite, including primary thickness, thermal diffusivity of the ash, and some other boundary conditions. The authors documented the influence of the glass composition and computed the mutual influence of two successive flow units. The model calculations show a density maximum within the centre of each flow unit separated from the other by a density low, the intensity of which depends mainly on the pause in deposition. When we apply this model of polymodal density distribution to the İncesu ignimbrite, we can infer that the İncesu ignimbrite is a compound cooling unit composed of at least three flows or, better said, emplacement units.

In a first approximation, we can further estimate emplacement temperatures and original depositional thicknesses from the SiO_2 content of the glass shards and the maximum density of the deposit at the type section. We might expect a deposit of 40 m of uncompacted thickness deposited at ± 720 °C (Riehle *et al.* 1995, p. 327, Figure 8).

In addition, the overall vertical density distribution – with the highest density most commonly near the base of the deposit – is consistent with the model of Sparks (1997) and Sparks *et al.* (1998). They propose that exsolved gasses trapped in the pore space of fresh tephra can be redissolved back into the glass of shards and pumice under the conditions of an increasing pressure regime of a compacting deposit. To support their model, those authors referred to frequent lack of gas-escape pipes and higher flattening of pumice relative to the deformation of glass shards in welded ignimbrites – characteristics that are also valid for the İncesu ignimbrite.

Lateral Density Variations

The model explanation here has to account chiefly for the principal differences between the northwestern Himmetdede lobe and the southern Firaktin-Hoşca lobe.

Pyroclastic flows propagate easily several tens of kilometres from their source vents and are able to surmount topographic barriers hundreds of meters high (Bursik & Woods 1996). The experiments of Woods *et al.* (1998) showed that the sedimentation patterns associated with ridges of different sizes may be very different. Flows involving partial blocking and formation of upstream propagating bores in front of a large-scale ridge display enhanced sedimentation upstream from the ridge, analogous to valley-ponded and caldera-fill deposits. In contrast, if a flow is able to surmount a ridge, the deposits are relatively unaffected by the ridge.

These experiments provide a possible explanation for the observed density variation in the southern Firaktin-Hoşca lobe of the İncesu ignimbrite. Pyroclastic flows were obviously able to surmount the Hoşca Pass completely, in so far as characteristic valley-ponded thickening of the deposit is lacking on the northern slope of the Hoşca Pass. Down ridge, the observed thickening (and degree of welding) at location 88 is thought to represent a deposit of lee-side concentration after dilution of the pyroclastic flow. The southernmost location (109) represents the blocking of the flows in front of the Taurus Mountains. The observed relatively dense welding is interpreted in terms of compression of the stopped flow combined with partial backflow from the upper slopes. The resultant overthickening of the deposit is made responsible for the high degree of welding according to the models of Riehle *et al.* (1995) and Sparks *et al.* (1998).

Summary and Conclusions

The İncesu ignimbrite is identified in the field by its welding intensity and its zoned changes in colour throughout its distribution area. Changes in colour correspond to variations in modal composition. The areal distribution of the ignimbrite is strongly controlled by palaeotopography that channelised individual flow portions and partly terminated their runout, especially in the Taurus forehills. However, distinct valley ponds are rare.

The vertical pattern of welding intensity shows a polymodal distribution in bulk rock density that is not obvious from field observation. The type section in the town of İncesu and, similarly, the entire distribution area except for the south – southeastern lobes, has its highest bulk rock density in the lower part of the deposit and shows an upward decrease that is superposed by 1 – 3 subordinate density maxima. The lateral variation of welding intensity discriminates two different types of distribution lobes which can be typified by the NW – Himmetdede lobe and the S – Firaktin-Hoşca lobe. The northwestern lobe is not terminated by topographic

barriers at its distal end and shows a constant decrease in bulk rock density, from proximal dense welding to distal incipient/non-welding. The southern lobe overtopped the 200 m elevation of the Hoşca Pass and finally came to rest in front of the Taurus Mountains. In contrast to the Himmetdede area, the location at the distal end of the Firaktin-Hoşca lobe exhibits a higher bulk rock density than locations along the spreading path.

The İncesu ignimbrite was emplaced by massive pyroclastic flows which preserved a temperature above the welding threshold. Welding in general occurred as compaction welding after the flows came to rest, and apparently no secondary flow occurred during the welding process. The polymodal distribution of bulk rock density indicates that the İncesu ignimbrite is multiple, composed of several flow and emplacement units which are separated from each other by short pauses in deposition and, thus, perhaps also in extrusive activity. Each emplacement unit reached the welding threshold as indicated by the various density peaks which are separated from each other by lows corresponding to intermittent pauses.

Welding may have been promoted by volatile redissolution such that, under compaction of the deposit by its own weight, the bulk rock density is highest in the lower parts. The relatively high bulk rock densities at the distal ends of topographically terminated flows are explained by the formation of bores in front of the barrier and partial backflow from the slopes. These bores and backflows caused overthickening of the deposit and thereby a higher degree of compaction and, consequently, higher bulk rock density.

Acknowledgements

A detailed study of the İncesu ignimbrite was initiated by Ulrike Mues-Schumacher some time ago when she recognised distinct vertical and lateral variations in rock density. Petra Lepetit performed the studies on the influence of modal composition on the bulk rock density as part of her master's thesis supervised by Lothar Viereck-Götte. He further facilitated XRF-analyses of samples from remote locations to identify and discriminate the İncesu ignimbrite from overlying deposits during an earlier stage of the project. We all are grateful to our Turkish colleagues, particularly Vedat Toprak of Middle East Technical University, Ankara, for their logistical support and help in exporting the samples to Germany. The manuscript benefited greatly from a thorough review with helpful comments by Anita Grunder, Abidin Temel and Asuman Türkmenoğlu who courteously reviewed the manuscript for this journal.

References

Bursik, M.I. & Woods, A.W. 1996. The dynamics and thermodynamics of large ash flows. *Bulletin of Volcanology* **58**, 175–193.

Chapin, C.E. & Lowell, G.R. 1979. Primary and secondary flow structures in ash-flow tuffs of the Gribbles Run Paleovalley, Central Colorado. *Geological Society of America Special Paper* **180**, 137–154.

Innocenti, F., Mazzuoli, R., Pasquarè, G., Radicati di Brozolo, F. & Villari, L. 1975. The Neogene calcalkaline volcanism of Central Anatolia: geochronological data on Kayseri – Niğde area. *Geological Magazine* **112**, 349–360.

Kürkcüoğlu, B., Şen E., Aydar, E., Gourgaud, A. & Gündoğdu, N. 1998. Geochemical approach to magmatic evolution of Mt. Erciyes stratovolcano Central Anatolia, Turkey. *Journal of Volcanology and Geothermal Research* **85**, 473–494.

Le Pennec, J.L. , Temel, A., Camus, A., Bourdier, J.L. & Gourgaud, A. 1991. Stratigraphy and source areas of the Neogene ignimbrites of Cappadocia (central Turkey). *International Conference on Active Volcanoes and Risk Mitigation, Napoli, Abstracts* (unpaginated).

Le Pennec J.L., Bourdier J.L., Froger J.L., Temel A., Camus G. & Gourgaud, A. 1994. Neogene ignimbrites of the Nevşehir plateau (central Turkey): stratigraphy, distribution and source constraints. *Journal of Volcanology and Geothermal Research* **63**, 59–87.

Lepetit, P. 1999. *Ursachen der Dichtevariation im Verschweißungsprofil des İncesu Ignimbrits, Zentralanatolien.* MSc Thesis, Friedrich-Schiller-Universität, Jena – Germany [in German, unpublished].

Mues-Schumacher, U. 1997. The İncesu ignimbrite – a large volume welded ignimbrite from central Anatolia. *IAVCEI International Volcanological Congress*, Puerto Vallarta – Mexico, Abstracts, p. 133.

Mues-Schumacher, U. & Schumacher, R. 1996. Problems of stratigraphic correlation and new K-Ar data for ignimbrites from Cappadocia, Central Turkey. *International Geological Review* **38**, 737–746.

Pasquarè, G. 1968. Geology of the Cenozoic volcanic area of Central Anatolia. *Atti Della Accademia Nazionale Dei Lincei* **9**, 53–204.

PASQUARÈ, G., POLI, S., VEZZOLI, L. & ZANCHI, A. 1988. Continental arc volcanism and tectonic setting in Central Anatolia, Turkey. *Tectonophysics* **146**, 217–230.

PETERSON, D.W. 1979. Significance of the flattening of pumice fragments in ash flow tuffs. *Geological Society of America Special Paper* **180**, 195–204.

RAGAN, D.M. & SHERIDAN, M.F. 1972. Compaction of the Bishop tuff, California. *Geological Society of America Bulletin* **83**, 95–106.

RIEHLE, J.R. 1973. Calculated compaction profiles of rhyolitic ash-flow tuffs. *Geological Society of America Bulletin* **84**, 2193–2216.

RIEHLE, J.R., MILLER, T.F. & BAILEY, R.A. 1995. Cooling, degassing and compaction of rhyolitic ash flow tuffs: a computational model. *Bulletin of Volcanology* **57**, 319–336.

SCHUMACHER, R., KELLER, J. & BAYHAN, H. 1990. Depositional characteristics of ignimbrites in Cappadocia, Central Anatolia, Turkey. *In*: SAVAŞÇIN, M.Y. & ERONAT, A.H. (eds), *Proceedings of the International Earth Sciences Congress on Aegean Regions (IESCA 1990)* Volume II, 435–449.

SCHUMACHER, R. & MUES-SCHUMACHER, U. 1996. The Kızılkaya ignimbrite – an unusual low-aspect-ratio ignimbrite from Cappadocia, central Turkey. *Journal of Volcanology and Geothermal Research* **70**, 107–121

SCHUMACHER, R. & MUES-SCHUMACHER, U. 1997. The pre-ignimbrite (phreato)plinian and phreatomagmatic phases of the Akdağ-Zelve ignimbrite eruption in Central Anatolia, Turkey. *Journal of Volcanology and Geothermal Research* **78**, 139–153.

SHERIDAN, M.F. 1979. Emplacement of pyroclastic flows: a review. *Geological Society of America Special Paper* **180**, 125–136.

SMITH, R.L. 1960a. Ash-flows. *Geological Society of America Bulletin* **71**, 795–842.

SMITH, R.L. 1960b. Zones and zonal variations in welded ash-flows. *US Geological Survey Professional Paper* **354F**, 49–159.

SMITH, R.L. 1979. Ash-flow magmatism. *Geological Society of America Special Paper* **180**, 5–27.

SMITH, R.L. & BAILEY, R.A. 1965. The Bandelier Tuff: a study of ash-flow eruption cycles from zoned magma chambers. *Bulletin of Volcanology* **29**, 83–104.

SPARKS, R.S.J. 1997. Origin of densely welded rocks by volatile dissolution. *IAVCE-I International Volcanological Congress, Puerto Vallarta – Mexico, Abstracts*, p. 140.

SPARKS, R.S.J., TAIT, S.R. & YANEV, Y. 1998. Dense welding caused by volatile resorption. *Journal of the Geological Society of London* **156**, 217–225.

STRECK, M.J. & GRUNDER, A.L. 1995. Crystallization and welding variations in a widespread ignimbrite sheet; the Rattlesnake Tuff, eastern Oregon, USA. *Bulletin of Volcanology* **57**, 151–169.

TEMEL, A. 1992. *Kapadokya Eksplozif Volkanizmasının Petrolojik ve Jeokimyasal Özellikleri [Petrological and Geochemical Characteristics of the Cappadocian Explosive Volcanism]*. PhD Thesis, Hacettepe University, Ankara–Turkey [in Turkish with English abstract, unpublished].

TEMEL, A., GÜNDOĞDU, M.N., GOURGAUD, A. & LEPENNEC, J.L. 1998. Ignimbrites of Cappadocia (Central Anatolia, Turkey): petrology and geochemistry. *Journal of Volcanology and Geothermal Research* **85**, 447–471

TOPRAK, V., KELLER, J. & SCHUMACHER, R. 1994. *Volcano-tectonic Features of the Cappadocian Volcanic Province*. IAVCE-I International Volcanological Congress, Ankara-Turkey Excursion Guide, 1–58.

VIERECK-GÖTTE, L., LEPETIT, P., SCHUMACHER, R. & MUES-SCHUMACHER, U. 2001. Sources of regular density variations within the welded İncesu ignimbeite / Cappadocia. *Fourth International Turkish Geology Symposium, Adana–Turkey, Abracts,* p. 317.

WALKER, G.P.L. 1983. Ignimbrite types and ignimbrite problems. *Journal of Volcanology and Geothermal Research* **17**, 65–88.

WOODS, A.W., BURSIK, M.I. & KURBATOV, A.V. 1998. The interaction of ash flows with ridges. *Bulletin of Volcanology* **60**, 38–51.

Received 22 July 2003; revised typescript accepted 15 March 2004